Infectious Disease Modelling 10 (2025) 229–239

Contents lists available at ScienceDirect

Infectious Disease Modelling

journal homepage: www.keaipublishing.com/idm

Network-based virus dynamic simulation: Evaluating the fomite disinfection effectiveness on SARS-CoV-2 transmission in indoor environment

Syun-suke Kadoya [a, *], Sewwandi Bandara [b], Masayuki Ogata [c], Takayuki Miura [d], Michiko Bando [d], Daisuke Sano [b, e, **]

[a] Department of Urban Engineering, The University of Tokyo, 7-3-1, Hongo, Bunkyo-ku, Tokyo, 113-8656, Japan
[b] Department of Frontier Science for Advanced Environment, Graduate School of Environmental Studies, Tohoku University, Sendai, Miyagi, 980-8572, Japan
[c] Department of Architecture, Faculty of Urban Environmental Sciences, Tokyo Metropolitan University, Hachioji, Tokyo, 192-0397, Japan
[d] Department of Environmental Health, National Institute of Public Health, Wako, Saitama, 351-0197, Japan
[e] Department of Civil and Environmental Engineering, Graduate School of Engineering, Tohoku University, Sendai, Miyagi, 980-8579, Japan

ARTICLE INFO

Article history:
Received 19 January 2024
Received in revised form 4 June 2024
Accepted 20 October 2024
Available online 22 October 2024
Handling Editor: Dr. Jianhong Wu

Keywords:
SARS-CoV-2
Disinfection
Indoor environment
Fomite
Network analysis
Virus transmission dynamics

ABSTRACT

Severe acute respiratory syndrome coronavirus 2 (SARS-CoV-2) is involved in aerosol particles and droplets excreted from a coronavirus disease 2019 (COVID-19) patient. Such aerosol particles or droplets including infectious virions can be attached on fomite, so fomite is not a negligible route for SARS-CoV-2 transmission within a community, especially in indoor environment. This necessarily evokes a need of fomite disinfection to remove virions, but the extent to which fomite disinfection breaks off virus transmission chain in indoor environment is still elusive. In this study, we evaluated the fomite disinfection effectiveness on COVID-19 case number using network analysis that reproduced the reported indoor outbreaks. In the established network, virus can move around not only human but also air and fomite while growing in human and decaying in air and on fomite, and infection success was determined based on the exposed virus amount and the equation of probability of infection. The simulation results have demonstrated that infectious virions on fomite should be kept less than a hundred to sufficiently reduce COVID-19 case, and every-hour disinfection was required to avoid stochastic increase in the infection case. This study gives us a practical disinfection manner for fomite to control SARS-CoV-2 transmission in indoor environment.

* Corresponding author.
** Corresponding author.
E-mail addresses: kadoya.s.ns@niph.go.jp (S.-s. Kadoya), daisuke.sano.e1@tohoku.ac.jp (D. Sano).
Peer review under responsibility of KeAi Communications Co., Ltd.

https://doi.org/10.1016/j.idm.2024.10.004

1. Introduction

Severe acute respiratory syndrome coronavirus 2 (SARS-CoV-2), which causes a predominantly respiratory illness, has spread worldwide in an instance after the first outbreak of coronavirus disease 2019 (COVID-19) in Wuhan, China (Zhou et al., 2020). SARS-CoV-2, mainly found in samples obtained from patient's throat and lung (Wölfel et al., 2020), transmits airborne in aerosol particles and droplets involved in cough and sneeze of a COVID-19 patient (Morawska & Cao, 2020; Patel et al., 2020; Wang et al., 2020; Zhao et al., 2022). This leads a great deal of countries to introduce non-pharmaceutical intervention measures, such as wearing masks and physical distancing, which can lessen the risk of exposure to infectious virions, in order to mitigate the human-to-human transmission of SARS-CoV-2 (Brauner et al., 2021; Chu et al., 2020; Worby et al., 2020).

In addition to human-to-human transmission, there is a potential of infection via fomite contaminated with SARS-CoV-2 involved in aerosols and droplets, which can be high especially in indoor environment (Kraay et al., 2021; Pitol & Julian, 2021). This possibility can be supported by previous observations that SARS-CoV-2 RNA has been detected at various objects such as furniture, door handle, mobile phone and so on (Marcenac et al., 2021; Moore et al., 2021). Furthermore, there are implications of fomite-to-human transmission reported by previous studies. In an animal experiment, the disease manifestation by fomite transmission was observed although its severity was milder than airborne transmission (Port et al., 2021). A modeling study has demonstrated that fomite transmission is responsible for 30% of COVID-19 cases in the Diamond Princess Cruise ship outbreak (Azimi et al., 2021). In some medical settings, fomite transmission is definitely associated with high risk of infection (Jones, 2020; Kraay et al., 2021; Mizukoshi et al., 2020). SARS-CoV-2 is reportedly persistent up to several days depending on initial titer on fomite per touched area (Geng & Wang, 2022), indicating that an intervention measure should be also applied to fomite to keep high hygiene level and prevent SARS-CoV-2 transmission in indoor environment.

Disinfection, one of nonpharmaceutical intervention measures, is obviously significant to manage fomite-mediated SARS-CoV-2 transmission in indoor environment. SARS-CoV-2 has an envelope protein outside of the nucleocapsid protein (Wang et al., 2020), which is known to be disrupted by alcohol (Pfaender et al., 2015). Some of loci on envelope and capsid proteins can be also reactive to chlorine which has been widely used at not only medical facilities but also household (Castaño et al., 2021). Physical disinfection like ultraviolet irradiation damaging viral nucleic acid is also effective to SARS-CoV-2 inactivation (Silke et al., 2020). A lot of disinfection studies have proven that SARS-CoV-2 on fomite can be easily and completely inactivated by various disinfection approaches. However, the extent to which fomite disinfection reduces the number of COVID-19 cases and appropriate disinfection manner remains elusive.

In the present study, we evaluated the effectiveness of fomite disinfection on SARS-CoV-2 transmission using network-based simulation. We focused on three reports relevant to indoor COVID-19 outbreaks as SARS-CoV-2 transmission scenarios and reproduced these scenarios on hypothetical networks composed of three node types: human, atmosphere and fomite nodes. We simulated SARS-CoV-2 transmission among three nodes on the established networks and tracked the change in COVID-19 case number under various fomite disinfection settings (periodic disinfection and prior disinfection). The simulation results have shown that the prior disinfection, which determines the initial infectious titer on fomite, dominantly contributes to prevention of SARS-CoV-2 transmission. The periodic disinfection (*i.e.*, fomite disinfection every hour following prior disinfection) had smaller effect on the SARS-CoV-2 transmission than the prior disinfection, but importantly stochastic increase in COVID-19 case was inhibited by keeping on breaking off one of sources of transmission chain. The sensitivity analysis enabled us to derive the targeted log reduction value (otherwise, the acceptable virus amount) on fomite that should have been achieved. Our study can provide us an insight into the appropriate fomite disinfection manner in indoor environment not only for SARS-CoV-2 but also for emerging pathogens.

2. Methods

2.1. Outbreak scenarios

We employed three scenarios to simulate SARS-CoV-2 transmission and evaluated the fomite disinfection efficiency. All the outbreaks occurred in January 2020 in China. The first scenario (Scenario A) was associated with an outbreak at a restaurant, in which 89 users and four staffs stayed and a primary infected person generated nine secondary cases (Fig. 1A) (Li et al., 2021). In the restaurant, there were 18 tables (there were no users in one of the tables) and one toilet. Latter scenarios were relevant to SARS-CoV-2 outbreaks in buses. In the second scenario (Scenario B), 47 users were getting on the bus and seven secondary cases were reported (Fig. 1B) (Cheng et al., 2022). There were 50 seats and a toilet in the bus. As for the third scenario (Scenario C), SARS-CoV-2 spread during about 2-h round bus trip and the 2-h worship event, resulting in 23 COVID-19 cases out of 68 users from a primary case (Fig. 1C) (Tambyah et al., 2020). We just focused on SARS-CoV-2 transmission during the bus trip in Scenario C. There were 69 seats but no toilet in the bus. Users stayed for approximately two, three and 2 h on average under Scenario A, B and C, respectively.

2.2. Network construction

We postulated that SARS-CoV-2 infection succeeded via three transmission routes: direct transmission from a primary infected to a susceptible person (human-to-human transmission), indirect transmission through atmosphere in which infectious virions were moved from an infected (atmosphere-to-human transmission), and indirect transmission through

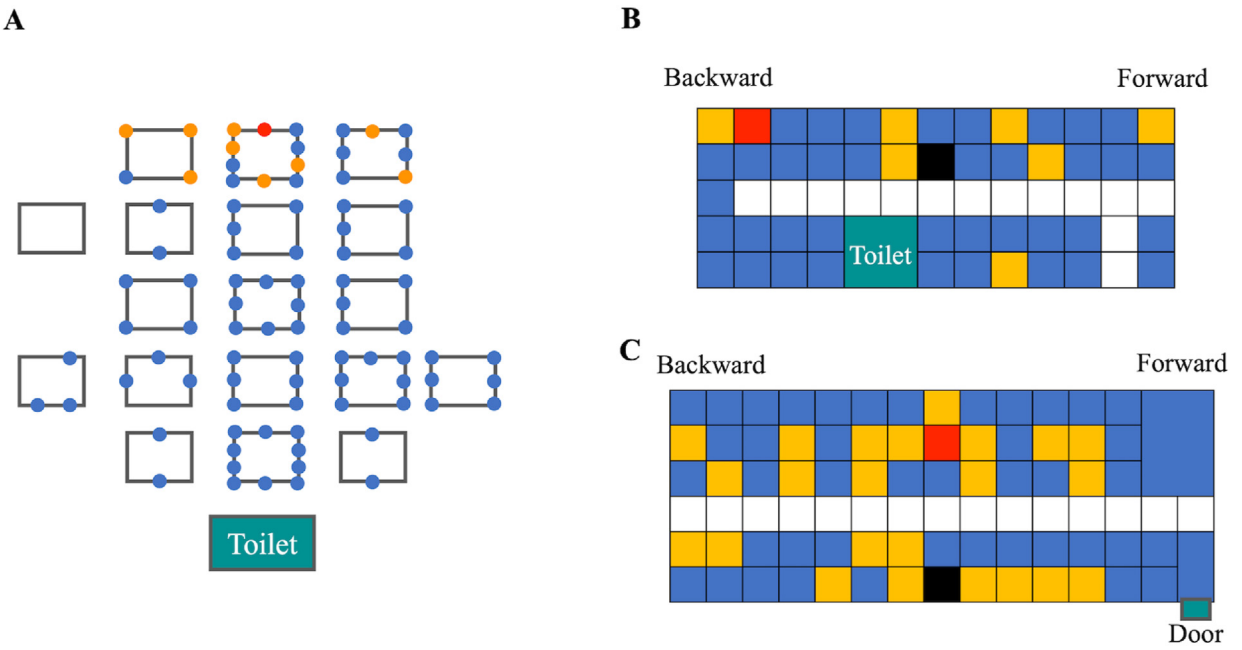

Fig. 1. Simplified diagrams for three COVID-19 outbreaks in indoor environment (A: Scenario A at restaurant, B: Scenario B at bus, C: Scenario C at bus). Blue, red and yellow cells show that non-infected, primary infected and secondary infected persons, respectively. Black and white cells mean vacant seats and a pathway in the bus.

fomite contaminated with SARS-CoV-2 (fomite-to-human transmission). To express these multiple transmission routes and reproduce transmission chains under three outbreak scenarios, we here applied the network analysis. The network is constructed based on "nodes" which are bridged between them with "links". In this study, users, assumed atmosphere blocks and common place (Scenario A, B: toilet, Scenario C: doorknob of the doorway) were assigned to human, atmosphere and fomite nodes, respectively. The links between human nodes were disposed based on information on family because they could talk face to face with each other, possibly causing direct virus transmission. To depict the atmosphere-to-human transmission, we considered the atmospheric node responsible for indirect transmission between family and non-family members. The atmospheric node was allocated according to space between tables in Scenario A (Fig. 1A), resulting in 24 atm nodes. A human node shares the neighbor atmosphere node with its non-family member (*i.e.*, human in different tables). In Scenario B, we partitioned left and right sides of two bus seat lines into three parts (forward, center and backward) (Fig. 1B) and thus assumed 6 atm nodes, which could be shared between family and non-family members who stayed in identical parts in the bus. In Scenario C, more atmosphere nodes (15 nodes) were assigned than Scenario B because the bus size was large and air masses could be stabilized at each location due to non-stop long bus trip where all passengers kept on sitting. We regarded a toilet surface or a doorknob of the doorway as a fomite node because these places were commonly and frequently utilized by users. Furthermore, the link between human and fomite nodes was determined by the assumption that at least one person in groups formed by connection around 1 atm node accessed the fomite node. These factitious networks were developed using the R package "igraph" (Csardi & Nepusz, 2006) under R software version 4.4.2 (https://www.r-project.org/).

2.3. Indicator of the network structure

We calculated *edge density* formulated as the actual number of links/the possible link number (*i.e.*, *edge density* corresponds to whole link number if all nodes are connected), to confirm whether the network was sparse or dense. In addition, the degree distribution exhibiting the number of links per a node was visualized. To evaluate a possibility that virus remained in and circulated over a small community, *transitivity*, namely whether a node "A" was linked with node "C" linking with node B adjacent to the node "A" (*i.e.*, whether three nodes formed a triangle), was calculated as the ratio of the triangle count and the number of triads including the case that a node "A" linked both with "B" and "C" but node "B" and "C" were not connected with each other. Furthermore, we calculated three types of *centrality* indicators to identify the node that could play a significant role in virus transmission. *Closeness centrality* is the reciprocal ratio of the averaged distance (the number of links to achieve the node) from all nodes to the number of nodes. This can indicate that the network has important central nodes that can scatter virus due to a lot of direct and indirect links with others. As with *edge density*, *degree centrality* is simply calculated based on the number of links but just implies that a central node can be responsible for infection of adjacent node. *Eigenvector centrality* can be estimated based on the assumption that the node connected with a central node is important. For example, a

human node with a few links is connected with an atmosphere node where many virions can be migrated. In this case, due to connection with a highly contaminated node, the human node is of importance for virus spread. All indicators of the network structure were calculated using the R package "igraph" (Csardi & Nepusz, 2006) under R software version 4.4.2 (https://www.r-project.org/).

2.4. Growth and decay of SARS-CoV-2

To reproduce actual SARS-CoV-2 transmission event, we assumed that a primary infected person was already at the stage of symptom onset and excreted infectious virions, indicating SARS-CoV-2 could grow in a human node. SARS-CoV-2 growth parameters were estimated by fitting the logistic equation for SARS-CoV-2 growth to the previously reported dataset using maximum likelihood estimation (Hou et al., 2020). The logistic equation is expressed as below:

$$\dot{V} = rV\left(1 - \frac{V}{K}\right) \quad \text{(Eq. 1)}$$

where V is the infectious titer-based virus amount [plaque forming unit at time t (PFU_t)], r is the specific growth rate [$hour^{-1}$], and K is the carrying capacity [$PFU_{t\to\infty}$]. The time course change in SARS-CoV-2 amount on a human node i is formulated using the difference equation along with the estimated r:

$$V_i[t] = \left\{1 + r\left(1 - \frac{V_i[t-1]}{K}\right)\right\}V_i[t-1] \quad \text{(Eq. 2)}$$

where V_i [t] is virus amount in a human node i at time t [hour]. We also assumed that SARS-CoV-2 infectivity declined on atmosphere and fomite nodes j due to natural decay:

$$V_j[t] = (1-k)V_j[t-1] \quad \text{(Eq. 3)}$$

where k is the natural decay constant [$hour^{-1}$]. The decay constants on atmosphere and fomite were 8.0 x 10^{-2} and 2.5 x 10^{-3} [$hour^{-1}$], respectively (Riddell et al., 2020; van Doremalen et al., 2020).

2.5. The network virus transmission dynamics

Direct (human-to-human transmission) and indirect (atmosphere- or fomite-to-human transmission) transmissions were simulated on the established network. SARS-CoV-2 in a node can move to the neighbor nodes via links. In the present study, we considered that viral amount migrating to a human node determined the probability of infection. SARS-CoV-2 can propagate on a human node while decaying in an atmosphere or a fomite node. The detailed algorithm for simulation of virus transmission is described below.

The established, undirected network object includes information on which nodes a node i is adjacent to and can be converted to an adjacent matrix A (if a node j is adjacent to a node i, namely there is a link between node i and node j, the entry a_{ji} of A is 1). To simulate virus transmission on the network, we developed an algorithm based on the adjacent matrix; (1) The network object was converted to the adjacent matrix. (2) To add information on which nodes virus existed, which human nodes the person had not experienced infection and how many virions the node had to the adjacent matrix A, three index vectors for them were prepared (non-infected vector S, virus-existing vector E and virus-amount vector X). (3) At the initial time step ($t = 0$), one of components of the virus-existing vector was assigned to 1, corresponding to a primary infection case. Also, initial virus amount V_0 was assigned to a fomite node under the assumption that the fomite was contaminated with virus prior to simulation start. (4) The inner product between A and E was calculated to get the number of infected and/or virus-contaminated nodes which were adjacent to the node i. (5) If the node i had some adjacent nodes that virus existed, information on virus amount was extracted, and then total amount of virus moving to the node i was calculated:

$$V_i = Log_{10}\left(\beta \sum v_j\right) \quad \text{(Eq. 4)}$$

where β is virus migration rate and v_i is virus amount on the adjacent nodes j that virus exists. The migration rate β was back-calculated using the previously reported distant-dependent probability of infection P and its equation ($\acute{\beta} = log\,(1-P)^{-1}$) (Agrawal & Bhardwaj, 2021). The $\acute{\beta}$ reported by the previous study has been termed the fraction of virus amount in patient's expiration, which was inhaled by a susceptible person (Agrawal & Bhardwaj, 2021), so the $\acute{\beta}$ can correspond to the proportion of the amount of migrated virus to node i to that of virus excreted from node j (termed β in this study). We also assumed that a person kept distance from 0.5 to 1.0 m from each other, and thus β was estimated based on the average between $\acute{\beta}(p = p(0.5))$ and $\acute{\beta}(p = p(1.0))$, resulting in β of approximately 0.4. Due to limitation of the study for virus transmission from environment to human, the β was also utilized as substitute for it. (6) The probability of SARS-CoV-2 infection establishment p_i increased as the virus amount migrated to node i was high:

$$p_i = 1 - (1 - p_0)^{V_i} \quad \text{(Eq. 5)}$$

where p_0 is the basic probability of infection per an event that a person exposes to an infectious virion, assumed to be 0.1 in the present study. (7) Whether infection succeeded or failed was determined based on binomial probability with the estimated p. If the binomial function for node i yielded 1, 1 was added to the component i of E whereas 1 was replaced from 0 in the component i of S. (8) After adding the migrated virus amount to X at t, the amount of virus migrated to human node at previous time step t -1 increased based on (Eq. (2)). On the other hand, (Eq. (3)) was applied to consider natural decay of virus on atmosphere and fomite nodes. (9) Finally, the processes (1)–(8) were repeated five times, equivalent to 5 h. Our simulation involves stochastic changes in virus transmission routes and viral amount because infection success depends on the binomial function (see Eq. (5) and the algorithm (7)), so simulation was run 100 times to consider stochastic variation of virus transmission route and subsequent infection case number.

2.6. Evaluation of the fomite disinfection efficiency

Two disinfection approaches were assumed here: “periodic” and “prior” disinfection. A fomite node was disinfected every hour by the periodic disinfection, thereby completely removing virions from a fomite node. Simulation without periodic disinfection was also performed to compare infection case numbers between presence and absence of periodic disinfection. We assumed that a fomite node was contaminated with 10^7 infectious virions at the beginning of simulation: however, the prior disinfection then altered initial virus amount on the fomite according to the set log reduction value (LRV). We compared infection case numbers when LRV by prior disinfection was 0 (*i.e.*, no reduction) and 7 (*i.e.*, all virions were inactivated). Furthermore, both disinfection approaches were concurrently performed to evaluate its effectiveness. Finally, to identify an appropriate disinfection strategy for the hypothetical situation, we performed sensitivity analysis in which frequency of periodic disinfection (every hour, once during simulation, no disinfection) and LRV by prior disinfection (from zero to seven LRV) varied.

3. Results and discussion

3.1. Description of the established networks

The network under Scenario A is composed of 118 nodes (93 human, 24 atm and 1 fomite nodes) and 765 links (Fig. 2a). Because the *edge density* is 0.08 (if all nodes are connected, the *edge density* is 1), the network is sparse, indicating the possibility that not all human nodes are likely infected. The degree distribution exhibits that approximately 80% nodes have more than five links (Fig. 2b), implying that virus can immediately spread once virus achieved the central node gathering a lot of links. This implication is further supported because *transitivity* is 0.72 indicating that virus can indirectly transmit to even distant nodes. The *eigenvector centrality* distribution is remarkably different from other centrality indicators (Fig. 2c): the fat-tailed shape implies that a few nodes connecting to central one is responsible for superspreading-based transmission. It is well-known that superspreading event is the dominant cause of SARS-CoV-2 secondary transmission (Sneppen et al., 2021), so the result of *eigenvector centrality* shows that we can reproduce practical SARS-CoV-2 transmission event using the established network.

The networks of bus scenarios (Scenario B and C) are smaller than that of restaurant scenario since there are 54 nodes with 114 links and 84 nodes with 183 links under Scenario B and C, respectively (Fig. 2d and g). *Edge density* values are 0.06 and 0.04 under Scenario B and C, respectively, and modes of their degree distribution are concentrated on less than three (Fig. 2e and h), which indicates that they are also sparse networks. In addition, lower *transitivity* of Scenario B (0.40) and C (0.29) than that of Scenario A can render outbreak sizes small. However, similar to Scenario A, *eigenvector centralities* form fat-tailed distributions (Fig. 2f and i). The nodes with high *eigenvector centrality* involve fomite nodes in all scenarios, making us easy to evaluate the fomite-disinfection effectiveness on preventing virus transmission. Taken together, all networks in this study are expected to realize practical SARS-CoV-2 transmission in each indoor environment and be useful to evaluate the disinfection effectiveness. Note that a fomite node is implicitly assumed to be the major factor of SARS-CoV-2 spread upon easily evaluating fomite-disinfection effectiveness.

3.2. Reproducibility of the developed network and effectiveness of periodic disinfection

The number of COVID-19 cases was followed up under simulation conditions with and without periodic disinfection for fomite every hour. Here, high initial infectious virions on fomite per touched area were set to 10^7. In Scenario A, the simulated case number at actual stay length (=2 h stay at the restaurant) was 10.7 on average, which was compatible to the reported secondary case (Fig. 3A). The network simulation for Scenario B also worked well since the estimated average case of 8.2 was similar to the reported one (Fig. 3B). On the other hand, in the case of Scenario C, the estimated case number of 6.4 on average was largely deviated from the confirmed case number (Fig. 3C): however, its inconsistency is not a matter because SARS-CoV-2 infection can also occur during the worship trip.

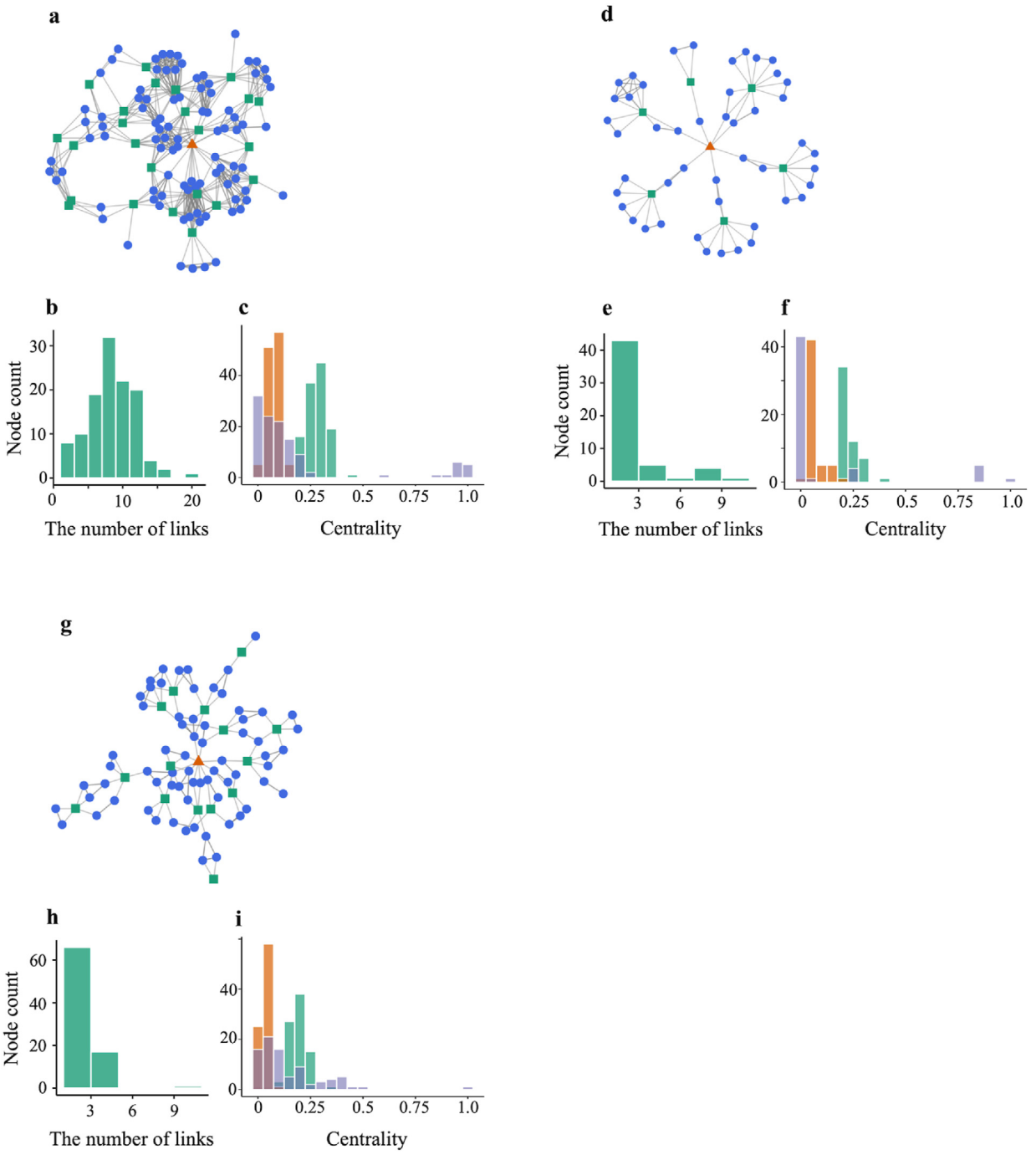

Fig. 2. The established network structures for Scenario A, B and C (a, d and g, respectively), and network indictors (b, c, e, f, h and i). (a, d, g) Nodes colored with blue, green and orange mean human, atmosphere and fomite nodes, respectively. Nodes are bound via links (grey line) that can be regarded as SARS-CoV-2 transmission routes. (b, e, h) *Edge density* distributions for Scenario A, B and C, respectively. (c, f, i) Three centrality indicators (green: *degree centrality*, orange: *closeness centrality*, blue: *eigenvector centrality*) for Scenario A, B and C, respectively.

Periodic disinfection is likely to have low capacity to mitigate the number of COVID-19 case. In the restaurant network simulation, the COVID-19 case number did not decrease nevertheless of periodic disinfection (Fig. 3A). On the other hand, the periodic disinfection slightly reduced the number of COVID-19 case in both bus scenarios, which came into prominence especially when simulation continued over actual stay length (Fig. 3B–C). The difference between restaurant and bus scenarios may come from the *edge density* (Fig. 2b, e and 2h). The number of links per a node is high in the restaurant network

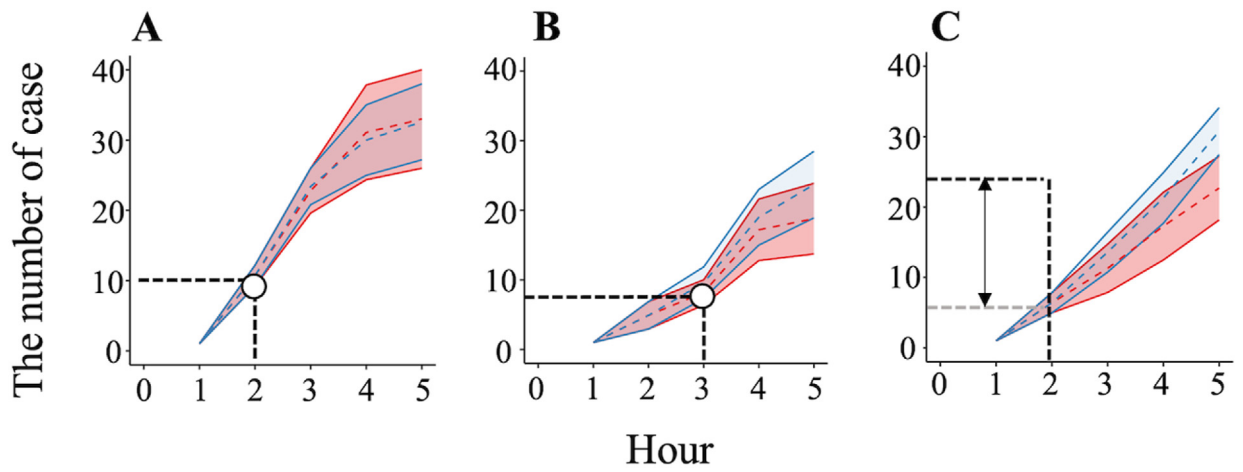

Fig. 3. Time course change of COVID-19 case in Scenario A, B and C to confirm the effectiveness of periodic disinfection. Dashed lines colored with blue and red show the averaged case numbers with and without periodic disinfection, respectively. Shade indicates the standard deviation. White circle indicates that the simulated value at the actual stay length is compatible to the actual case number. Only in Scenario C, the simulated value is deviated from practical one (indicated as an arrow) probably because virus transmission occurs during not only bus trip but also the accompanied worship event.

compared to bus networks, indicating that once virus on an infected or a contaminated node moves to the adjacent node, virus can immediately spread over the network and after that periodic disinfection cannot arrest the transmission chain until virus reaches the fomite node again. In fact, a lot of viruses can easily spread in this simulation condition because of high initial virus amount on fomite per touched area. Therefore, we need to assess whether initial contamination level on fomite, which is controlled by strict disinfection measure (*i.e.*, prior disinfection in this study), affects the outbreak size.

3.3. *Effectiveness of prior disinfection*

We here compared the expected COVID-19 case number under simulation conditions with and without prior disinfection by which all viruses were completely inactivated. In Scenario A, 76.7 % reduction in infection case number at the actual stay length was confirmed owing to prior disinfection (Fig. 4A). The result of simulation under Scenario B also showed that prior disinfection greatly impacted on the number of cases (79.1 % reduction; Fig. 4B). The largest reduction in COVID-19 case was confirmed under Scenario C (84.4% reduction; Fig. 4C). These results suggest that managing contamination level at the potential source is critical to prevent SARS-CoV-2 transmission in indoor environment. However, as the simulation time went

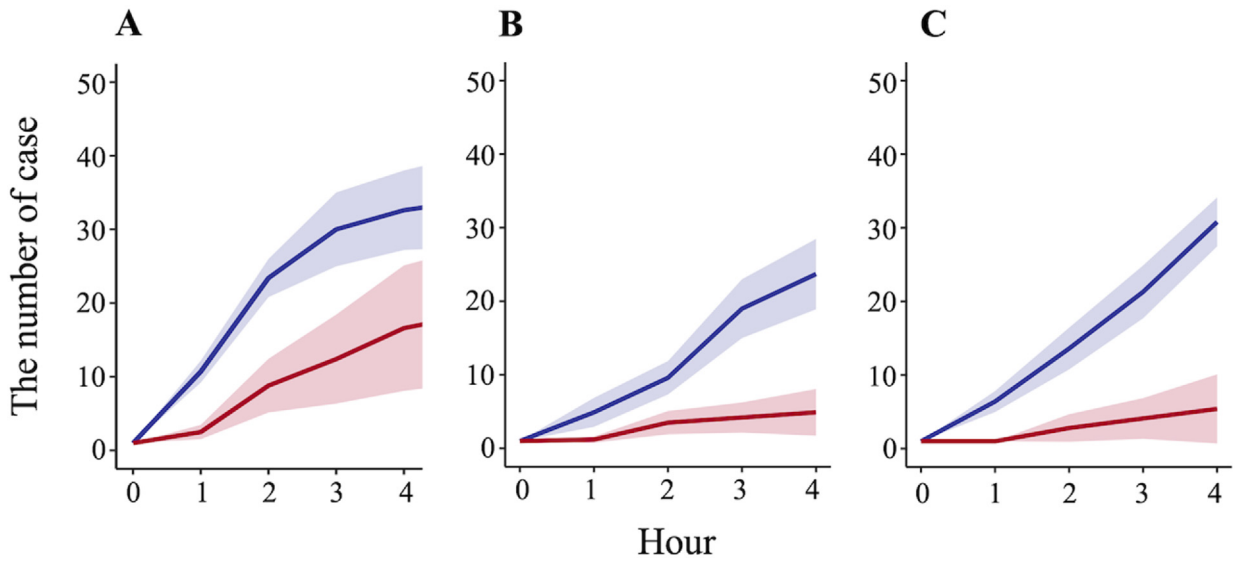

Fig. 4. The effect of prior disinfection on the number of infection case (A: Scenario A, B: Scenario B, C: Scenario C). Red and blue lines show the transition of averaged COVID-19 case with and without prior disinfection, respectively. Shade indicates the standard deviation.

on, we found that uncertainty of COVID-19 case number increased in all simulations with prior disinfection (Fig. 4). This is in particular attributable to recontamination with virus on the fomite node. When a fomite node is contaminated again with SARS-CoV-2 following the prior disinfection, the node returns to one of sources of virus transmission in the network. Therefore, it remains still insufficient to manage virus transmission over indoor environment only by the prior disinfection which corresponded to the scene like that common place is cleaned once just before passengers go on board.

3.4. Need of both disinfection approaches to shrink outbreak size

We then assessed the synergistic effect of prior and periodic disinfections because prior disinfection only could mitigate the early spread of SARS-CoV-2 (Fig. 4). We expected that periodic disinfection was effective if a fomite node was recontaminated after prior disinfection. Simulations were run under the condition that no virus existed on fomite due to prior disinfection in the beginning and then the subsequent periodic disinfection was conducted every hour. As shown in Fig. 5, in spite of periodic disinfection, slight increases in the infection case were found, which can result from human- or atmosphere-to-human transmission. On the other hand, periodic disinfection made the standard deviation of the infection case number small although averaged values were not so different from results of no periodic disinfection. This result indicates that periodic disinfection is eventually important to prevent stochastic increase in the COVID-19 case number, especially when viruses on a fomite node is incompletely removed by prior disinfection. In terms of practical application of disinfection and variety of disinfection methods and conditions, it can be difficult to always achieve the complete virus removal from fomite by disinfection (String et al., 2021; Viana Martins et al., 2022). In addition, there is no report suggesting the target LRV sufficient to mitigate virus transmission via fomite, making us difficult to propose an appropriate disinfection manner in indoor environment.

3.5. Sensitivity analysis

Sensitivity analysis was performed to determine the target LRV (that is, the acceptable viral amount on fomite per touched area) and the frequency of periodic disinfection. We compared the number of COVID-19 cases at actual stay length between three periodic disinfection manners (every hour, once during simulation and no disinfection) as LRV on a fomite node was changed, which was equivalent to variation of initial virus amount in the fomite node. As a result, in Scenario A, we found that COVID-19 case was rapidly dropped at 5 LRV (*i.e.*, 100 infectious virions on fomite per touched area) and afterwards was kept constant (Fig. 6A). This tendency was also seen in the other scenarios (Fig. 6B–C). The cause of sudden decrease in COVID-19 case can reside in that infection from fomite to human cannot succeed due to small viral amount that makes probability of infection too low to establish subsequent transmission chain (see Eq. (5)). Every-hour periodic disinfection slightly reduced the averaged case number and led its standard deviation downward at low LRV, indicating that periodic disinfection can be useful to mitigate infection case number even if prior disinfection yields lower LRV than expected due to accidental consumption of chemical disinfectant (Gang et al., 2003; Kadoya et al., 2019, 2021; Sohn et al., 2004). The standard deviation at more than 5 LRV especially in Scenario A and C was also made small by every-hour periodic disinfection (Fig. 6), which was compatible to the previous result (Fig. 5). Taken together, the sensitivity analysis has suggested that LRV should be adjusted so that the number of infectious virions on fomite per touched area can be less than a hundred and disinfection should be

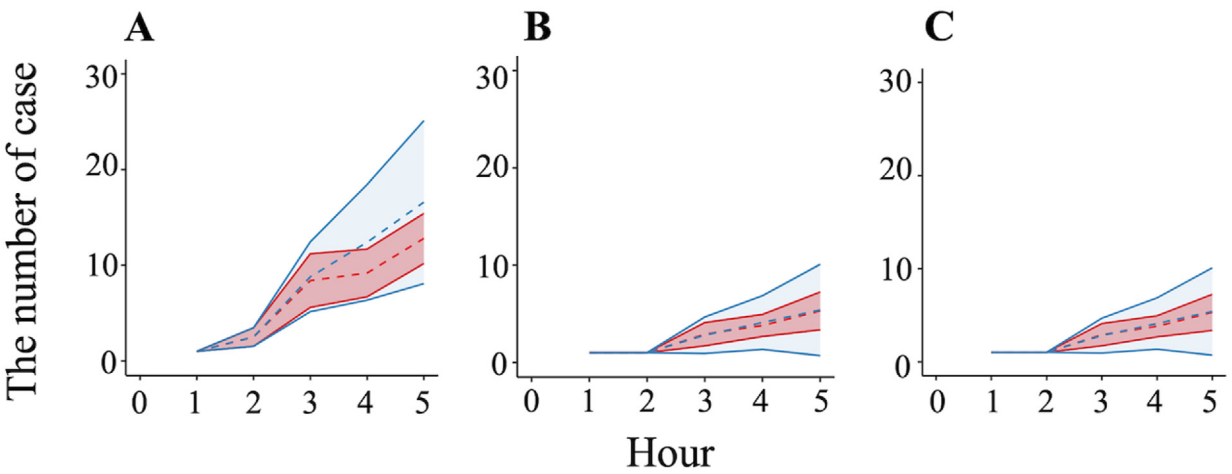

Fig. 5. The synergistic effect of prior and disinfections on the COVID-19 case number (A: Scenario A, B: Scenario B, C: Scenario C). Red and blue dashed lines show the transition of averaged COVID-19 case with and without periodic disinfection, respectively. Shade indicates the standard deviation.

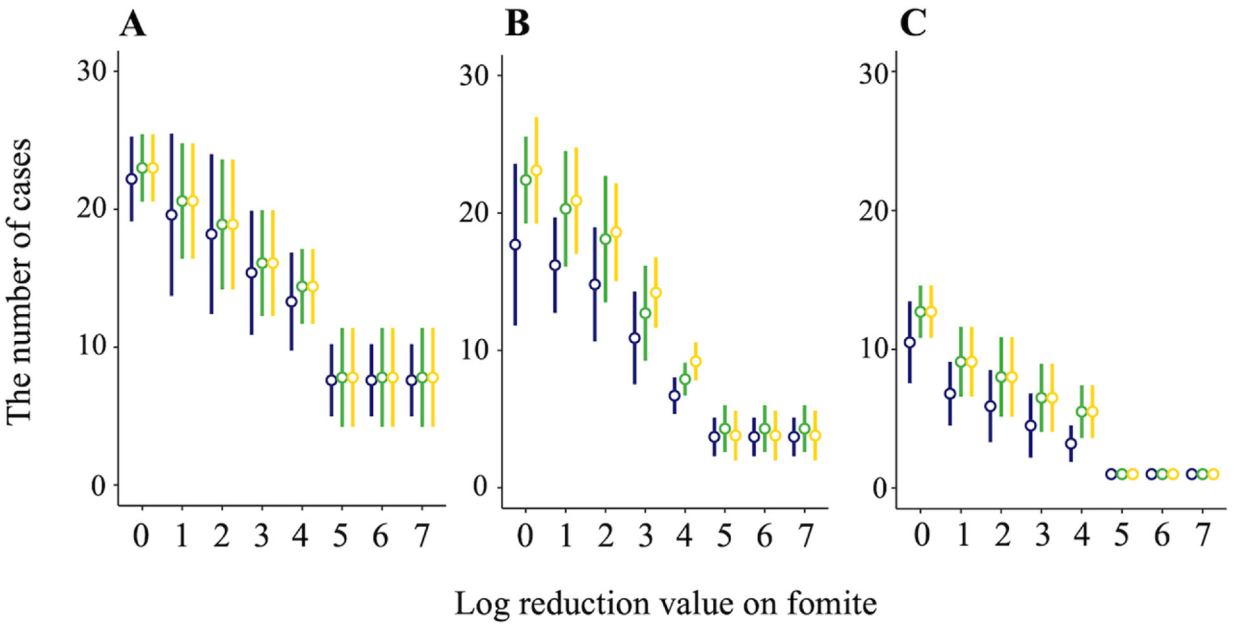

Fig. 6. Change in the COVID-19 case number under different periodic disinfection approach (navy: every hour, green: only once during simulation time, yellow: no periodic disinfection) and log reduction value by prior disinfection on fomite (A: Scenario A, B: Scenario B, C: Scenario C). The initial infectious titer of SARS-CoV-2 was 10^7 in this simulation. Circle and the error bar mean the average value and standard deviation, respectively.

conducted every hour to supplement a previously conducted disinfection that can be sometimes insufficient to achieve the targeted LRV.

3.6. Limitations and implications

This simulation study using network-based simulation has demonstrated that the prior disinfection plays a dominant role in inhibiting SARS-CoV-2 transmission before a user get into indoor environment and the number of infectious virions on fomite per touched area should be kept less than a hundred copy by prior and periodic disinfections. However, there are several limitations that should be declared.

First, the developed networks have just partially depicted actual outbreak situations since our aim is to evaluate the fomite disinfection effectiveness in a simple way. Virus transmission on the network started when all users stayed at their seats: however, in fact, SARS-CoV-2 must spread during each user entering the restaurant or getting on board. In regard to this, accidental contacts to other users must have happened in real situation. To reproduce more actual situation, the time-varying network, in which a human node temporally links non-family member nodes especially during boarding or going the assigned table at the restaurant, should be established in the further study. The links of an atmospheric node is also time-varying because air mass as an atmosphere node can be flown in a practical indoor environment. As for fomite node, there can be more than one fomite node in each scenario in practice, and frequency of contact with a fomite node should be taken into account in the future study.

Second, the network model did not reflect the practical ventilation condition and its effect on virus spread although atmospheric nodes we prepared in the networks enabled virus to move to the neighbor nodes. Ventilation has been widely known as an important intervention measure at present, and recent outbreak may have occurred in an indoor environment in which ventilation system is properly operated. In this case, our network model cannot reproduce virus transmission in the indoor environment. We need to employ a directed link of an atmospheric node and reconsider how atmospheric nodes are linked to human and other atmospheric nodes to express current situation of virus spread on the directed airflow. Note that ventilation or airflow effect is not critical for our simulation cases because previous studies have indicated that ventilation rate was poor and the indoor environments were crowded (Cheng et al., 2022; Li et al., 2021). We thus assumed that viruses were not carried on the directed airflow to a distant node and just prepared hypothetical atmospheric nodes, in which virus temporally stayed and could spread to adjacent nodes. This transition from an atmospheric node may be explained by diffusion and non-directed, weak airflow due to an air conditioner. Actually, our simulation, especially for scenarios A and B, successfully expressed the actual number of infection cases.

Third, we have assumed that virus migration rate β is identical between human-to-human, human-to-atmosphere, human-to-fomite transmissions and vice versa. This is because the rates for each transmission have not been estimated anywhere although some studies for fomite-associated transmission have employed the migration rate of surrogate viruses

(King et al., 2021), or focused on finger-initiated transfer of virus (Todt et al., 2021). In addition, it still remains unclear how many and how long infectious virions in aerosols and droplets stay in atmosphere. The β can also change depending on airflow condition in the indoor environment. To make virus transmission dynamics more actual, an experimental study which can estimate the migration rate or relative importance (Short & Cowling, 2023) among each transmission route is required.

Finally, this study has simulated virus transmission under rough disinfection condition, which always yields constant LRVs. However, the disinfection efficiency reportedly differs between disinfectants or fomite materials or contact time (Viana Martins et al., 2022). Also, variation of disinfection action, such as wipe, radiation and spray, may affect the LRV of SARS-CoV-2 on fomite. A comprehensive, experimental study for fomite disinfection is needed to determine the detailed disinfection condition (*e.g.*, contact time, concentration of disinfectant and disinfection action).

Although the enumerated limitations here must be considered in the further study to reproduce practical outbreak situation, the modeling and simulation concept can be useful to understand the indoor COVID-19 outbreak that will happen in the future and to estimate risk of infection in hospital, kindergarten and so on. Quantitative microbial risk assessment (QMRA) has been applied so far to estimate the risk of SARS-CoV-2 infection and disease burden in various scenarios (Dada & Gyawali, 2021; Denpetkul et al., 2022; Zhang et al., 2022). The network-based virus transmission model established here can track viral amount to which a human is exposed and can be also applied to evaluate the effect of wearing mask and physical distancing by modifying virus migration rate. Therefore, along with network-based simulation, the QMRA approach can enable us to evaluate whether the introduced non-pharmaceutical interventions are preventive for virus transmission in indoor environment, based on the estimated risk and the deviation between the estimated and targeted LRVs (or estimated and acceptable viral amounts). Taken together, the network virus transmission model and its concept can be conducive to describing viral outbreak situation and suggesting appropriate intervention measures.

4. Conclusion

SARS-CoV-2 infection succeeds via not only human-to-human transmission but also virus-contaminated fomite route. Disinfection used for keeping high hygiene level on fomite can be valuable to control SARS-CoV-2 transmission especially in indoor environment. However, fomite disinfection effectiveness on infection case number has not been investigated well. We here simulated SARS-CoV-2 transmission in indoor environments based on the network analysis and found that strict disinfection manner for fomite (i.e., less than a hundred virions on fomite was kept by prior and periodic disinfection) broke off the transmission chains, leading to drastic decrease in the infection case. Our modeling framework is also applicable to understanding the effect of non-pharmaceutical intervention measures, such as ventilation and social distancing, and can help us manage better indoor environment where pathogenic virus is hard to spread by combination with quantitative microbial risk analysis.

CRediT authorship contribution statement

Syun-suke Kadoya: Writing – original draft, Visualization, Methodology, Investigation, Formal analysis, Data curation, Conceptualization. **Sewwandi Bandara:** Investigation, Data curation. **Masayuki Ogata:** Writing – review & editing, Formal analysis. **Takayuki Miura:** Writing – original draft, Data curation. **Michiko Bando:** Writing – review & editing, Funding acquisition. **Daisuke Sano:** Writing – review & editing, Supervision, Project administration.

Declaration of competing interest

The authors declare that they have no known competing financial interests or personal relationships that could have appeared to influence the work reported in this paper.

Acknowledgements

This study was supported by MHLW Research on Health Security Control Program Grant Number JPMH21LA1007.

References

Agrawal, A., & Bhardwaj, R. (2021). Probability of COVID-19 infection by cough of a normal person and a super-spreader. *Physics of Fluids, 33*, Article 031704.

Azimi, P., Keshavarz, Z., Cedeno Laurent, J. G., Stephens, B., & Allen, J. G. (2021). Mechanistic transmission. modeling of COVID-19 on the diamond princess cruise ship demonstrates the importance of aerosol transmission. *Proceedings of the National Academy of Sciences, 118*(8), Article e2015482118.

Brauner, J. M., Mindermann, S., Sharma, M., Johnston, D., Salvatier, J., Gavenčiak, T., Stephenson, A. B., Leech, G., Altman, G., Mikulik, V., Norman, A. J., Monrad, J. T., Besiroglu, T., Ge, H., Hartwick, M. A., Yeh, Y. W., Chindelevitch, L., Gal, Y., & Kulveit, J. (2021). Inferring the effectiveness of government interventions against COVID-19. *Science, 371*, Article eabd9338.

Castaño, N., Cordts, S. C., Jalil, M. K., Zhang, K. S., Koppaka, S., Bick, A. D., Paul, R., & Tang, S. K. Y. (2021). Fomite. transmission, physicochemical origin of virus-surface interactions, and disinfection strategies for enveloped viruses with applications to SARS-CoV-2. *ACS Omega, 6*(10), 6509–6527.

Cheng, P., Luo, K., Xiao, S., Yang, H., Hang, J., Ou, C., Cowling, B. J., Yen, H.-. L., Hui, D. S. C., & Li, Y. (2022). Predominant airborne transmission and insignificant fomite transmission of SARS-CoV-2 in a two-bus COVID-19 outbreak originating from the same pre-symptomatic index case. *Journal of Hazardous Materials, 425*, Article 128051.

Chu, D. K., Akl, E. A., Duda, S., Solo, K., Yaacoub, S., & Schünemann, H. J. (2020). Physical distancing, face masks, and eye protection to prevent person-to-person transmission of SARS-CoV-2 and COVID-19: A systematic review and meta-analysis. *Lancet, 395*(10242), 1973–1987.

Csardi, G., & Nepusz, T. (2006). The igraph package for complex network research. *Int. J. Complex Systems, 1695*.
Dada, A. C., & Gyawali, P. (2021). Quantitative microbial risk assessment (QMRA) of occupational exposure to. SARS-CoV-2 in wastewater treatment plants. *Science of the Total Environment, 763*, Article 142989.
Denpetkul, T., Pumkaew, M., Sittipunsakda, O., Leaungwutiwong, P., & Sirikanchana, K. (2022). Effects of face. Masks and ventilation on the risk of SARS-CoV-2 respiratory transmission in public toilets: A quantitative microbial risk assessment. *Journal of Water and Health, 20*(2), 300–313.
Gang, C. E., Clevenger, T. E., & Baneriji, S. K. (2003). Modeling chlorine decay in surface water. *J. Environ. Inform., 1*, 21–27.
Geng, Y., & Wang, Y. (2022). Stability and transmissiblity of SARS-CoV-2 in the environment. *Journal of Medical Virology, 95*(1), Article e28103.
Hou, Y. J., Chiba, S., Halfmann, P., Ehre, C., Kuroda, M., Dinnon III, K. H., Leist, S. R., Schäfer, A., Nakajima, N., Takahashi, K., Lee, R. E., Mascenik, T. M., Graham, R., Edwards, C. E., Tse, L. P., Okuda, K., Markmann, A. J., Bartelt, L., de Silva, A., … Baric, R. S. (2020). SARS-CoV-2 D614G variant exhibits efficient replication ex vivo and transmission in vivo. *Science, 370*(6523), 1464–1468.
Jones, R. M. (2020). Relative contributions of transmission routes for COVID-19 among healthcare personnel. providing patient care. *Journal of Occupational and Environmental Hygiene, 17*(9), 408–415.
Kadoya, S., Nishimura, O., Kato, H., & Sano, D. (2019). Predictive water virology: Hierarchical Bayesian modeling. for estimating virus inactivation curve. *Water, 11*(10), 2187.
Kadoya, S., Nishimura, O., Kato, H., & Sano, D. (2021). Predictive water virology using regularized regression. analyses for projecting virus inactivation efficiency in ozone disinfection. *Water Research X., 11*, Article 100093.
King, M.-. F., Wilson, A. M., Weir, M. H., López-García, M., Proctor, J., Hiwar, W., Khan, A., Fletcher, L. A., Sleigh, A., Clifton, I., & Dancer, S. J. (2021). Modeling fomite-mediated SARS-CoV-2 exposure through personal protective equipment doffing in a hospital environment. *Indoor Air, 32*(1), Article e12938.
Kraay, A. N. M., Hayashi, M. A. L., Berendes, D. M., Sobolik, J. S., Leon, J. S., & Lopman, B. A. (2021). Risk for. Fomite-mediated transmission of SARS-CoV-2 in child daycares, schools, nursing homes, and offices. *Emerging Infectious Diseases, 27*(4), 1229–1231.
Li, Y., Qian, H., Hang, J., Chen, X., Cheng, P., Ling, H., Wang, S., Liang, P., Li, J., Xiao, S., Wei, J., Liu, L., Cowling, B. J., & Kang, M. (2021). Probable airborne transmission of SARS-CoV-2 in a poorly ventilated restaurant. *Building and Environment, 196*, Article 107788.
Marcenac, P., Park, G. W., Duca, L. M., Lewis, N. M., Dietrich, E. A., Barclay, L., Tamin, A., Harcourt, J. L., Thornburg, N. J., Rispens, J., Matanock, A., Kiphibane, T., Christensen, K., Pawloski, L. C., Fry, A. M., Hall, A. J., Tate, J. E., Vinjé, J., Kirking, H. L., & Pevzner, E. (2021). Detection of SARS-CoV-2 on surfaces in households of persons with COVID-19. *International Journal of Environmental Research and Public Health, 18*, 8184.
Mizukoshi, A., Nakama, C., Okumura, J., & Azuma, K. (2020). Assessing the risk of COVID-19 from multiple. Pathways of exposure to SARS-CoV-2: Modeling in health-care settings and effectiveness of nonpharmaceutical interventions. *Environment International, 17*(9), 408–415.
Moore, G., Rickard, H., Stevenson, D., Aranega-Bou, P., Pitman, J., Crook, A., Davies, K., Spencer, A., Burton, C., Easterbrook, L., Love, H. E., Summers, S., Welch, S. R., Wand, N., Thompson, K.-. A., Pottage, T., Richards, K. S., Dunning, J., & Bennett, A. (2021). Detection of SARS-CoV-2 within the healthcare environment: A multi-centre study conducted during the first wave of the COVID-19 outbreak in england. *Journal of Hospital Infection, 108*, 189–196.
Morawska, L., & Cao, J. (2020). Airborne transmission of SARS-CoV-2: The world should face the reality. *Environment International, 139*, Article 105730.
Patel, K. P., Vunnam, S. R., Patel, P. A., Krill, K. L., Korbitz, P. M., Gallagher, J. P., Suh, J. E., & Vunnam, R. R. (2020). Transmission of SARS-CoV-2: An update of current literature. *Eur. J. Clin. Microbiol. Infect., 39*, 2005–2011.
Pfaender, S., Brinkmann, J., Todt, D., Riebesehl, N., Steinmann, J., Steinmann, J., Pietschmann, T., & Steinmann, E. (2015). Mechanisms of methods for hepatitis C virus inactivation. *Applied and Environmental Microbiology, 81*(5), 1616–1621.
Pitol, A. K., & Julian, T. R. (2021). Community transmission of SARS-CoV-2 by surfaces: Risks and risk reduction. Strategies. *Environmental Science and Technology Letters, 8*(3), 263–269.
Port, J. R., Yinda, C. K., Owusu, I. O., Holbrook, M., Fischer, R., Bushmaker, T., Avanzato, V. A., Schulz, J. E., Martens, C., van Doremalen, N., Clancy, C. S., & Munster, V. J. (2021). SARS-CoV-2 disease severity and transmission efficiency is increased for airborne compared to fomite exposure in Syrian hamsters. *Nature Communications, 12*, 4985.
Riddell, S., Goldie, S., Hill, A., Eagles, D., & Drew, T. W. (2020). The effect of temperature on persistence of SARS-CoV-2 on common surfaces. *Virology Journal, 17*, 145.
Short, K. R., & Cowling, B. J. (2023). Assessing the potential for fomite transmission of SARS-CoV-2. *Lancet. Microbe., 4*(6), e380–e381.
Silke, H. C., Leonie, S., Oliver, W., Mira, A., Wilhelm, A. U., Ulf, D., Kathrin, S., Mirko, T., Dongliang, Y., Xin, Z., Eike, S., & Adalbert, K. (2020). Susceptibility of SARS-CoV-2 to UV irradiation. *American Journal of Infection Control, 48*(10), 1273–1275.
Sneppen, K., Nielsen, B. F., Taylor, R. J., & Simonsen, L. (2021). Overdispersion in COVID-19 increases the. effectiveness of limiting nonrepetitive contacts for transmission model. *Proceedings of the National Academy of Sciences, 118*(14), Article e2016623118.
Sohn, J., Amy, G., Cho, J., Lee, Y., & Yoon, Y. (2004). Disinfectant decay and disinfection by-product formation. model development: Chlorination and ozonation by-products. *Water Research, 38*, 2461–2478.
String, G. M., White, M. R., Gute, D. M., Mühlberger, E., & Lantagne, D. S. (2021). Selection of a SARS-CoV-2. surrogate for use in surface disinfection efficacy studies with chlorine and antimicrobial surfaces. *Environmental Science and Technology Letters, 8*, 11.
Tambyah, P. A., Conly, J., & Voss, A. (2020). Community outbreak investigation of SARS-CoV-2 transmission. among bus riders in eastern China. *JAMA Internal Medicine, 180*(12), 1665–1671.
Todt, D., Meister, T. L., Tamele, B., Howes, J., Paulmann, D., Becker, B., Brill, F. H., Wind, M., Schijven, J., Heinen, N., Kinast, V., Mhlekude, B., Goffinet, C., Krawczyk, A., Steinmann, J., Pfaender, S., Brüggemann, Y., & Steinmann, E. (2021). A realistic transfer method reveals low risk of SARS-CoV-2 transmission via contaminated euro coins and banknotes. *iScience, 24*(8), Article 102908.
van Doremalen, N., Morris, D. H., Holbrook, M. G., Gamble, A., Williamson, B. N., Tamin, A., Harcourt, J. L., Thornburg, N. J., Gerber, S. I., Lloyd-Smith, J. O., de Wit, E., & Munster, V. (2020). Aerosol and surface stability of SARS-CoV-2 as compared with SARS-CoV-1. *New England Journal of Medicine, 382*(16), 1564–1567.
Viana Martins, C. P., Xavier, C. S. F., & Cobrado, L. (2022). Disinfection methods against SARS-CoV-2: A systematic. Review. *Journal of Hospital Infection, 119*, 84–117.
Wang, Y., Xu, G., & Huang, Y.-. W. (2020a). Modeling the load of. SARS-CoV-2 virus in human expelled particles. during coughing and speaking. *PLoS One, 15*(10), Article e0241539.
Wang, M.-. Y., Zhao, R., Gao, L.-. J., Gao, X.-. F., Wang, D.-. P., & Cao, J.-. M. (2020b). SARS-CoV-2: Structure, biology, and structure-based therapeutics development. *Frontiers in Cellular and Infection Microbiology, 10*, Article 587269.
Wölfel, R., Corman, V. M., Guggemos, W., Selimaier, M., Zange, S., Müller, M. A., Niemeyer, D., Jones, T. C., Vollmar, P., Rothe, C., Hoelsher, M., Bleicker, T., Brünink, S., Shneider, J., Ehmann, R., Zwirglmaier, K., Drosten, C., & Wendtner, C. (2020). Virological assessment of hospitalized patients with COVID-2019. *Nature, 581*, 465–469.
Worby, C. J., Yang, X. L., & Wang, X. G. (2020). A pneumonia outbreak associated with a new coronavirus of. probable bat origin. *Nature, 579*, 270–273.
Zhang, X., Wu, J., Smith, L. M., Li, X., Yancey, O., Franzblau, A., Dvonch, J. T., Xi, C., & Neitzel, R. (2022). Monitoring SARS-CoV-2 in air and on surfaces and estimating infection risk in buildings and buses on a university campus. *Journal of Exposure Science and Environmental Epidemiology, 32*, 751–758.
Zhao, X., Liu, S., Yin, Y., Zhang, T., & Chen, Q. (2022). Airborne transmission of. COVID-19 virus in enclosed. spaces: An overview of research methods. *Indoor Air, 32*, Article e13056.
Zhou, P., Yang, X. L., & Wang, X. G. (2020). A pneumonia outbreak associated with a new coronavirus of probable. bat origin. *Nature, 579*, 270–273.